

Implementation of a PV Panel Model based on the Look-up Tables Method for a PV Generator Emulator

Manelle HASNAOUI

Université de Tunis El Manar,
Ecole Nationale d'Ingénieurs de Tunis,
LR11ES15 Laboratoire des Systèmes
Electriques, 1002, Tunis, Tunisie;
manelle.hasnaoui@enit.utm.tn

Afef BENNANI-BEN ABDELGHANI

Université de Tunis El Manar,
ENIT, LR11ES15, 1002, Tunis, Tunisie;
Université de Carthage, INSAT, Centre
Urbain Nord, 1080Tunis, Tunisie;
Afef.beanabdelghani@insat.rnu.tn

Ilhem SLAMA-BELKHODJA

Université de Tunis El Manar,
Ecole Nationale d'Ingénieurs de Tunis,
LR11ES15 Laboratoire des Systèmes
Electriques, 1002, Tunis, Tunisie;
ilhem.slama@enit.rnu.tn

Abstract—This paper deals with the design of a PV generator emulator for pre-certificated tests of solar inverters. The power topology is defined to meet standards requirements and provide the current versus voltage (I-V) curve under defined conditions of irradiation and temperature. The standard EN50530 related to overall efficiency of grid connected photovoltaic inverters gives the model of PV panel to be used. Thereby, an algorithm is proposed for model implementation on a low cost digital target (STM32F4), and also for power structure control in order to reproduce the PV panel behavior. Simulation and experimental results of a 60 W PV panel emulator are presented and discussed.

Keywords— Photovoltaic system, I-V photovoltaic module characteristic, PV Emulator, Look-up tables, test bench;

1. INTRODUCTION

The PV roof-top market is continuously growing and the performances of the PV grid connected systems are nowadays one of the major issues. The PV inverter is the heart of such systems and its performances strongly impact the whole system ones. They depend on both DC-DC and DC-AC conversion stages and on maximum power point tracking (MPPT) algorithm performances. For their evaluation, experimental tests have to be conducted according to the EN50530 standard. The performance evaluation could be performed using a PV generator (panels) or a programmable DC power source that reproduces the behavior of the PV generator under various conditions of irradiation and temperature. In this case, the PV generator model is given by standards and then the current versus voltage I-V relationship. Thus, this DC source should reproduce as closely as possible this model: its power structure has to act like a power amplifier and its control should ensure high dynamic performances under variables change.

Several researches have been conducted in this field. Some works have focused on converter topology and others on PV model to be implemented. Different topologies are proposed in the literature. PWM rectifier [1], diode rectifier and DC/DC buck converter[2], programmable DC power supply with resistive load [3], [4] are the most common ones. New topologies have been investigated like ZVS full-Bridge type [5]. Works related to PV model can be divided into two categories:

mathematical model giving I-V relationship [6]–[8] and its implementation methodology. The platform used for the implementation could be based on FPGAs [9], [10], dSPACE [11] or LabVIEW [12], whereas, model implementation methodology is generally based on look-up table [13], [14] or semiconductor physics equations [15], [16]. Model parameters could be those given by standards or by PV panel datasheets [17] or by dedicated algorithm.

Low cost implementation has been considered by some authors. The approach is generally based on the use of analog circuits to generate I-V curve, [18], [19].

This paper focuses on the use on a low cost solution based of STM32F4 for PV panel model and power converter control implementation. So, look-up table method has been selected and the paper details the algorithm derived from this approach. The emulator components are firstly presented and then the establishment of the look-up table from mathematical nonlinear equations is detailed. The approach is illustrated by simulation and experimentally validated with 60Wp PV panel model.

2. PV GENERATOR EMULATOR STRUCTURE

The PV emulator under study consists of two parts: power structure and its control. The control allows the power stage to imitate the operating performance of a PV generator and to fulfill the standard requirements. Fig. 1 represents the I-V and P-V curve that should be reproduced.

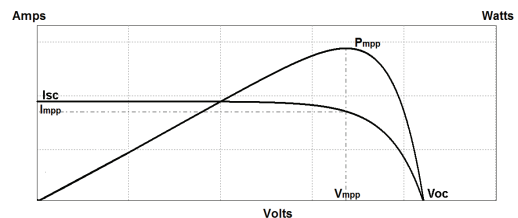


Fig. 1 I-V and P-V curves of a PV generator

A. Power topology

The H-bridge structure has been selected since it allows to reach extreme points such as the open-circuit voltage (V_{oc}) and the short-circuit current (I_{sc}) that

correspond respectively to zero current and zero voltage. Fig.2 shows the power structure of the PV generator emulator.

The H-bridge converter allows current and voltage reversibility, so very low and null current and voltage values could be reached (mean value after filtering).

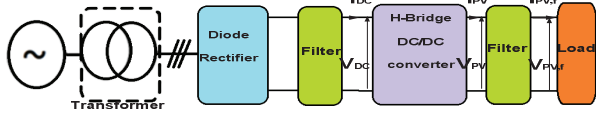


Fig. 2 Emulator power structure

An output LC filter has been designed to let current ripples within limits specified by standards. Fig.3 shows the current and voltage obtained with $L=60\text{mH}$ and $C=180\mu\text{C}$ with a $5\ \Omega$ resistive load under irradiation $G=200\text{W/m}^2$ and ambient temperature $T=25^\circ\text{C}$. The voltage ripples are the most challenging ones since before being filtered, the output voltage V_{pv} varies between 1500V and -1500V . These ripples are less than 0.5%.

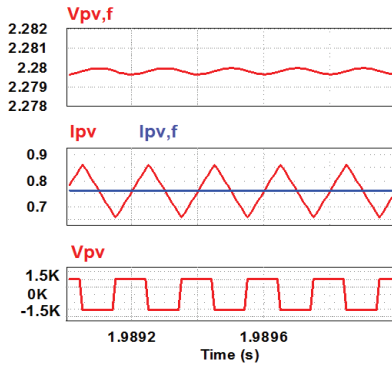


Fig. 3 H-Bridge output current and voltage, before ($I_{pv}; V_{pv}$) and after filtering ($I_{pv,f}; V_{pv,f}$)

B. Control approach

The control stage, illustrated in Fig. 4, is composed of three modules: PWM, current control and I-V curve generator. It requires filtered DC current and voltage measurements. The measured voltage is the input of I-V curve generator module which outputs then current value according to this curve. This value is the reference current I_{PV_ref} for the current control loop whereas PI regulator is designed using pole placement approach.

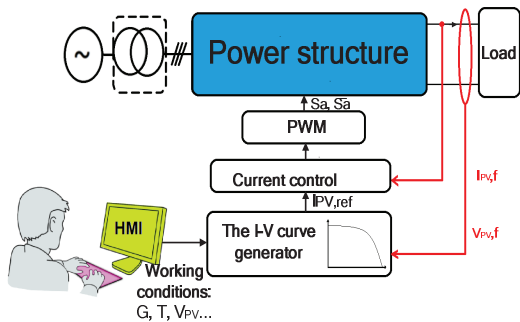


Fig. 4 PV generator emulator control principle

The low cost solution adopted is based on STM32F4 digital card. The three control modules and also conversion stages have to be implemented on this device. Fig.5 gives the detailed structure of proposed control for the PV emulator, where $V_{pv,f}$ and $I_{pv,f}$ are the analog emulator outputs $V_{pv,D}$ and $I_{pv,D}$ are the digital conversions of $V_{pv,f}$ and $I_{pv,f}$.

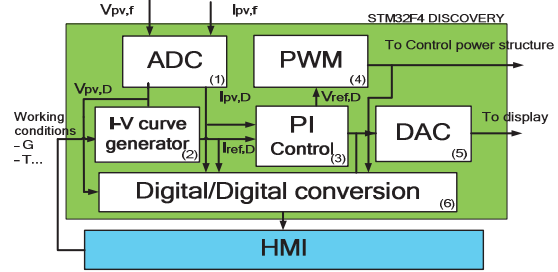


Fig. 5 Different modules of the proposed control for the PV emulator

C. Mathematical model

Standard EN 50530 dealing with the overall efficiency of grid connected photovoltaic inverters provides the I-V curve expression (1) to be implemented [20]. This equation is a mathematical nonlinear relationship between PV generator current and voltage integrating parameters depending on climatic conditions (irradiation G and temperature T), the emulated panel technology (Crystalline Silicon Cs_i , Thin-film TF ...) and data sheet parameters (current in short-circuit, I_{SC} and voltage open-circuit V_{OC} , maximum power point ratings under STC standards test conditions).

$$I_{PV} = I_{SC} - I_0 \left(e^{\frac{V_{PV}}{V_{OC} C_{AQ}}} - 1 \right) \tag{1}$$

where

- I_{PV} : PV generator current under operating
- I_{SC} : Short-Circuit current under operating conditions
- I_0 : Saturation current of the diode
- V_{PV} : PV generator voltage under operating conditions
- V_{OC} : Open-Circuit voltage under operating conditions

Variable C_{AQ} is a constant given by standard. It depends on current and voltage fill factors noted respectively FF_I and FF_V .

$$C_{AQ} = \frac{FF_V - 1}{\ln(1 - FF_I)} \tag{2}$$

$$I_{SC} = I_{SC,STC} \frac{G}{G_{STC}} (1 + \alpha (T_{PV} - T_{STC})) \tag{3}$$

$$I_0 = I_{SC,STC} (1 - FF_I)^{\frac{1}{1-FF_V}} \frac{G}{G_{STC}} \tag{4}$$

$$V_{OC} = V_{OC,STC} (1 + \beta (T_{PV} - T_{STC})) \left(\ln \left(\frac{G}{C_G} + 1 \right) C_V - C_{RG} \right) \tag{5}$$

G : Irradiation in operating conditions

- G_{STC} : Irradiation in the STC conditions (1000W/m²)
- T_{PV} : Temperature of PV module
- T_{STC} : Temperature in STC conditions (25°C)
- $I_{sc, stc}$: Short-Circuit current in STC conditions
- $V_{oc, stc}$: Open-Circuit voltage in STC conditions
- α : Current temperature coefficient
- β : Voltage temperature coefficient
- C_G, C_V, C_R : Correction Factors depending on panel technologies
- FF_I : Current fill factor
- FF_U : Voltage fill factor

With

$$FF_I = \frac{I_{MPP,STC}}{I_{sc, STC}} \quad (6)$$

$$FF_U = \frac{V_{MPP,STC}}{V_{oc, STC}} \quad (7)$$

where

$I_{MPP,STC}$: Maximum power point current in the STC conditions

$V_{MPP,STC}$: Maximum power point voltage in the STC conditions

The exponential function in (1) and logarithmic ones in (5) are to be implemented for real time and fast current control. The following section details the proposed solution to overcome problems related to the computing time these non linear functions. To this purpose, A and B are defined by (8) and (9).

$$A = e^{\frac{V_{PV}}{V_{oc}C_{AQ}} - 1} \quad (8)$$

$$B = \ln\left(\frac{G}{C_G} + 1\right) \quad (9)$$

The idea is to implement each of (A) and (B) expressions using a look-up table. Since two different technologies have to be used, 4 tables will be implemented on the target device

D. I-V relationship algorithm

Standard EN50530 requires values of seven parameters: α , β , C_G , C_V , C_R , FF_I and FF_U . They depend only on emulated PV panel technology. Each parameter have only one value chosen among two defined by standard according to the PV panel technology. All cases are then grouped in the vector (named *Parameter_Vector*) having two columns and seven rows.

depends on FF_I and FF_U i.e. only on PV panel technology. Thus C_{AQ} takes two values: one for the *Csi* technology and another for the *TF* technology. Therefore, the variation of the expression $(\frac{V_{PV}}{V_{oc}C_{AQ}} - 1)$ depends only on the variation of the ratio $(\frac{V_{PV}}{V_{oc}})$. This ratio, as expressed in (10) is always less than 1 since V_{PV} varies between 0 and V_{oc} .

$$0 \leq \frac{V_{PV}}{V_{oc}} \leq 1 \quad (10)$$

A look-up table has been defined to implement expression (A) defined in equation (8): Its length is limited by the STM32F4 memory resources. In our case, the maximum length is 3000 elements (float). Each index corresponds to $\frac{V_{PV}}{V_{oc}}(i)$, i varying from 1 to 3000.

For the implementation of expression (B) (given by equation (9)), irradiation G has to be considered. Indeed, C_G is a variable depending on PV panel technology and G varies from 0 to 1500 W/m².

Thereby, the look-up table dedicated to expression (B) implementation contains 1500 elements (integer); each one corresponds to an irradiation value.

Tables for expression (A) and (B) are named *Table_A* and *Table_B* respectively.

The organizational chart in Fig. 6 summarizes the proposed methodology.

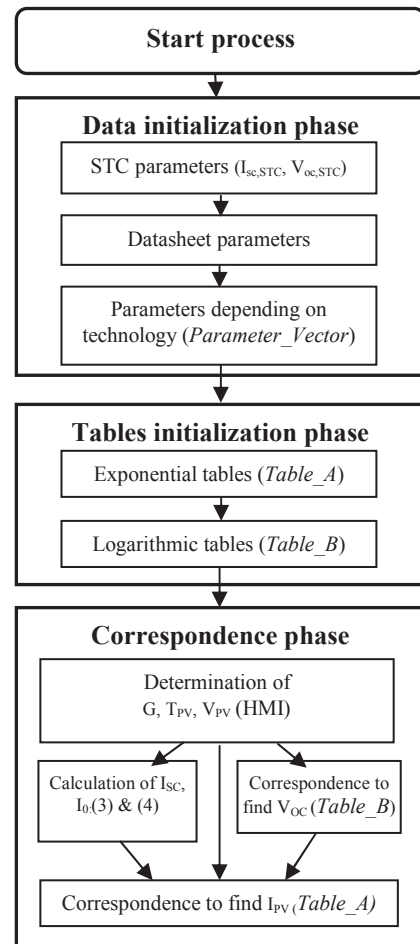


Fig. 6 Flowchart for the control

3. SIMULATION RESULTS C_{AQ}

Simulations are performed with PSIM software of POWERSYS. At first, only the I-V curve generator, using the look-up tables, is simulated and confronted to the mathematical expressions generator and also a PV panel modeling, offered by PSIM. Secondly, all the

system (power structure and control stages) are considered.

Studied PV panel characteristics are given in Table I:

TABLE I
PV panel characteristics

Variable	Value
Technology	: <i>Csi</i>
$V_{OC,STC}$	= 21.1 V,
$I_{SC,STC}$	= 3.8 A,
$V_{MPP,STC}$	= 17.1 V,
$I_{MPP,STC}$	= 3.5 A.

The first simulation gives the comparison between I-V curves based on look-up tables and model proposed by PSIM, under STC conditions.

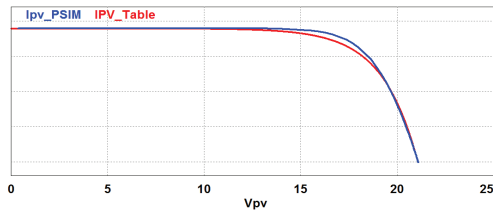


Fig. 7. Comparison between the I-V curve generator using table and PSIM model

Fig. 7 shows that the two curves are similar, except near to the maximum power point. This dissimilarity is result of FF_I and FF_U different values. The I_{pv_Table} in Fig.7 has been obtained using values imposed by standard ($FF_I = 0.9$ and $FF_U = 0.8$ for the *Csi* technology) whereas I_{pv_PSIM} current is obtained using PSIM model (calculated from PV panel datasheet).

Thereafter, in Fig. 8, I-V curve using look-up tables is compared to the one using mathematical expression, given by standard EN50530, for the same PV panel characteristics and the same operating conditions STC. These curves are well superimposed. The zoom shows the exponential function discretization effect due to table implementation.

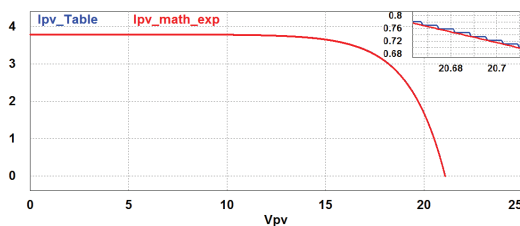


Fig. 8. Comparison between the I-V curve generator using table and mathematical model

Absolute error between them is evaluated using (11) and Fig.9 shows that this error, in STC conditions, does not exceed tens milliamps between the two curves.

$$\epsilon = |I_{pv,math,exp} - I_{pv,Table}| \quad (11)$$

Percent error δ is defined by (12) and (13) where ϵ_r is relative error between the two curves.

$$\epsilon_r = \frac{\epsilon}{|I_{pv,math,exp}|} \quad (12)$$

$$\delta = 100\% \cdot \epsilon_r \quad (13)$$

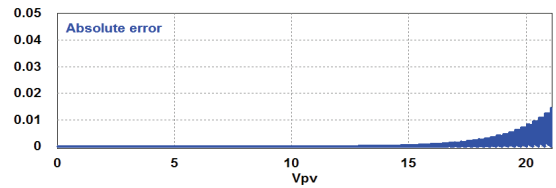


Fig. 9. Absolute error between the I-V curve generator using table and I-V using mathematical model

Percent error is less than 1% for 95% of the I-V curve, until $V_{pv}=20V$. Indeed, this expression could not be calculated for current values close to zero.

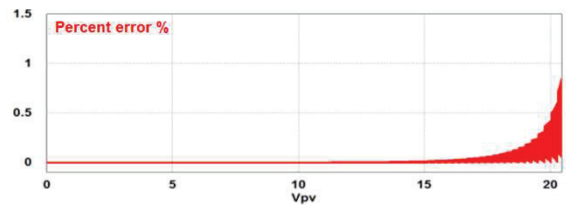


Fig. 10 Percent error between the I-V curve generator using tables and I-V using mathematical model

Impact of climatic parameters is tested using different G and T. Fig. 11 shows I-V curves under different irradiances and Fig. 12 gives absolute error between the two curves, for each irradiation: this absolute error decreases with irradiation.

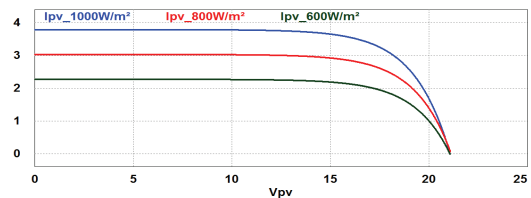


Fig. 11. Different I-V curves under different irradiances



Fig. 12. Absolute errors between the I-V curve generator using table and mathematical model for different irradiances

Fig. 13 shows I-V curves according to different temperature and Fig. 14 shows absolute error for each temperature.

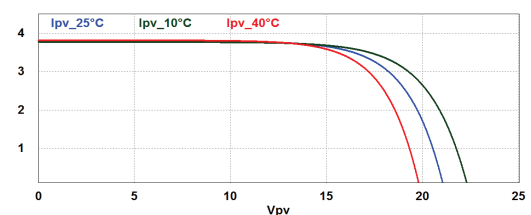


Fig. 13 Different I-V curves for different temperatures

The temperature change engenders error translation but has no effect on its magnitude.

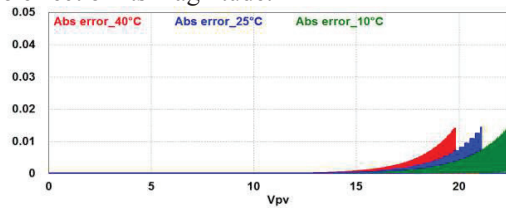


Fig. 14 Absolute errors between between the I-V curve generator using table and mathematical model for differents temperature

Simulating serial and parallel PV panel connection provides expected results as shown in Fig. 15 and Fig. 16.

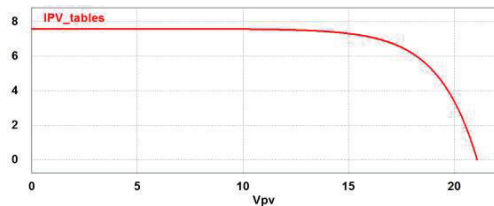


Fig. 15 The I-V curve for two PV panels connection in parallel

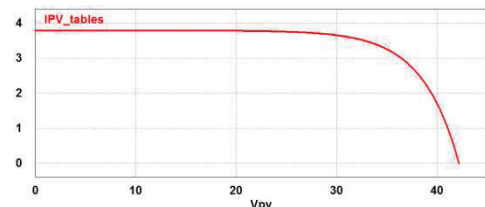


Fig. 16. The I-V curve for a connection in series of two panels

In this paper, authors do not focus on the current control, so this part is not detailed. Simulations have been conducted with power structure illustrated in Fig.2 and control stages shown in Fig.4. The resistive load is changed to reach desired operating points. In Fig 17, the continuous I-V curve is obtained using only the implemented I-V model, whereas each point corresponds to a steady state operating point obtained with the whole emulator (power stage and control stages). The results demonstrate the effectiveness of the proposed approach.

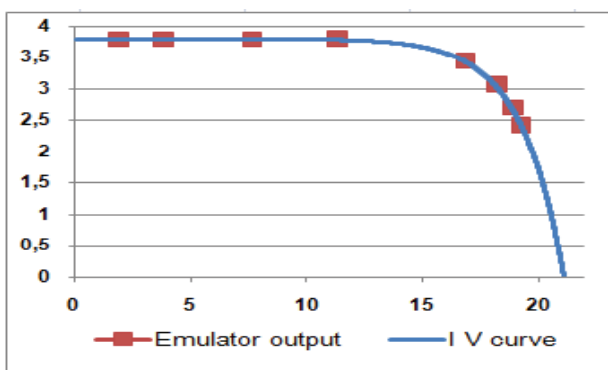


Fig. 17 Comparison between the theoretical I-V curve and emulator outputs for different values of resistive loads, under STC conditions

4. EXPERIMENTAL VALIDATION

Experimental validation has been performed with a laboratory testbench designed for a 6kVA PV emulator.

Table II gives its data and Fig. 18 details its different components. The first experimental tests have been conducted for studied PV panel (Table I).

TABLE II
Power structure components

Components	Characteristics
Three-phase transformer	6 kVA, m=2.6
Three-phase autotransformer	6 kVA, m=1
Three-phase diode rectifier	SKD 51/16, 1700V-50A
H-bridge DC/DC	SKM50GB1 2T4, 1200V, 50A
LC filter	L=60 mH, C=180 μF
R load	R=13.5 Ω, adjustable
Digital storage oscilloscope	MCP DQ8074

Interface board has been developed for STM32F4 board and IGBT driver voltage adaptation, and a sensor board groups current and voltage sensors.

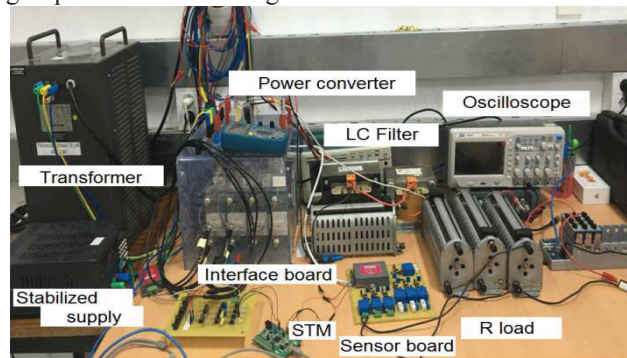


Fig. 18 Test bench of the PV generator emulator tests

The first test was to validate the I-V algorithm implementation : an external DC power supply provides a fixed voltage V_{PV} to the I-V curve generator, the output current I_{PV} , is displayed on the PC. In Fig.19, four V_{PV} experimental operating points are reported : $V_{PV,1}=5V$, $V_{PV,2}=10.5V$, $V_{PV,3}=14.7V$ and $V_{PV,4}=17.1V$. The output currents meet the desired I-V curve.

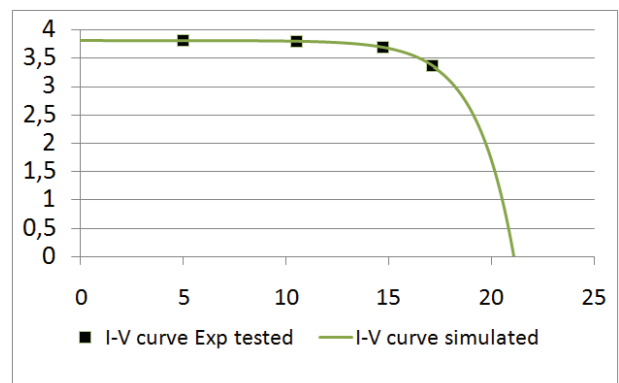


Fig. 19 I-V curve experimentally tested vs simulated I-V curve

Secondly, closed loop current control is tested. Results reported in Fig. 20 shows system response for different current references: 0.5 A, 2 A and 3 A. Each screen displays V_{dc} voltage in the DC bus, V_{pv} voltage in H-

bridge output and I_{pv} . Current response time is 10ms for all cases.

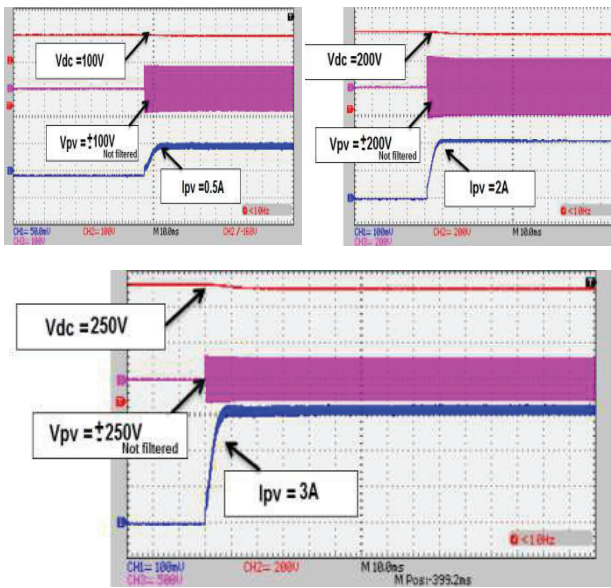


Fig. 20 Results of the current PI regulator tests

5. CONCLUSION

The paper presents allow cost PV panel model implementation to reproduce I-V curve, according to model defined by standard. The proposed algorithm is based on look-up tables. This approach allows to implement table instead of the model nonlinear expressions to minimize computing time. Simulations results give a percent error between tables method and analytic expression less than 1%. Experimental laboratory test bench has been developed and tests have been conducted for 60 Wp PV panel emulation. Experimental results demonstrate the effectiveness of the approach.

ACKNOWLEDGMENT

This work is under an ongoing project PNRI EC/ORE, directed by the CETIME (Mechanical and Electrical Industries Technical Center), with collaboration of SACEM Smart member of SACEM Group.

REFERENCES

[1] M. He, H. Liu, X. You, and T. Q. Zheng, "Research on photovoltaic array simulator based on the PWM rectifier," in *2009 IEEE Energy Conversion Congress and Exposition*, 2009, pp. 302–306.

[2] H. Qi, Y. Bi, and Y. Wu, "Development of a photovoltaic array simulator based on buck converter," in *2014 International Conference on Information Science, Electronics and Electrical Engineering (ISEEE)*, 2014, vol. 1, pp. 14–17.

[3] D. S. L. Dolan, J. Durago, and Taufik, "Development of a photovoltaic panel emulator using Labview," in *2011 37th IEEE Photovoltaic Specialists Conference (PVSC)*, 2011, pp. 001795–001800.

[4] A. F. Ebrahim, S. M. W. Ahmed, S. E. Elmasry, and O. A. Mohammed, "Implementation of a PV emulator using programmable DC power supply," in *SoutheastCon 2015*, 2015, pp. 1–7.

[5] J. P. Lee et al., "Development of a photovoltaic simulator with novel simulation method of photovoltaic characteristics," in *INTEEC 2009 -*

31st International Telecommunications Energy Conference, 2009, pp. 1–5.

[6] A. Tedeschi, F. R. Fulginei, and A. Laudani, "PV Panel Modeling: A Mobile Application for Modeling Photovoltaic Panels Using Datasheets Information," in *2015 3rd International Conference on Future Internet of Things and Cloud (FiCloud)*, 2015, pp. 608–613.

[7] A. Salman, A. Williams, H. Amjad, M. K. L. Bhatti, and M. Saad, "Simplified modeling of a PV panel by using PSIM and its comparison with laboratory test results," in *2015 IEEE Global Humanitarian Technology Conference (GHTC)*, 2015, pp. 360–364.

[8] L. H. I. Lim, Z. Ye, J. Ye, D. Yang, and H. Du, "A Linear Identification of Diode Models from Single Characteristics of PV Panels," *IEEE Trans. Ind. Electron.*, 2015, vol. 62, no. 7, pp. 4181–4193.

[9] G. M. Tornez-Xavier, F. Gómez-Castañeda, J. A. Moreno-Cadenas, and L. M. Flores-Nava, "FPGA development and implementation of a solar panel emulator," in *2013 10th International Conference on Electrical Engineering, Computing Science and Automatic Control (CCE)*, 2013, pp. 467–472.

[10] D. Ickilli, H. Can, and K. S. Parlak, "Development of a FPGA-based photovoltaic panel emulator based on a DC/DC converter," in *2012 38th IEEE Photovoltaic Specialists Conference (PVSC)*, 2012, pp. 001417–001421.

[11] A. Rachid, F. Kerrou, R. Chenni, and H. Djeghloud, "PV emulator based buck converter using dSPACE controller," in *2016 IEEE 16th International Conference on Environment and Electrical Engineering (EEEIC)*, 2016, pp. 1–6.

[12] S. Thale, R. Wandhare, and V. Agarwal, "A novel low cost portable integrated solar PV, fuel cell and battery emulator with fast tracking algorithm," in *2014 IEEE 40th Photovoltaic Specialist Conference (PVSC)*, 2014, pp. 3138–3143.

[13] A. Ilyas, M. R. Khan, and M. Ayyub, "Lookup table based modeling and simulation of solar photovoltaic system," in *2015 Annual IEEE India Conference (INDICON)*, 2015, pp. 1–6.

[14] Z. G. Piao, S. J. Gong, Y. H. An, and G. B. Cho, "A study on the PV simulator using equivalent circuit model and look-up table hybrid method," in *2013 International Conference on Electrical Machines and Systems (ICEMS)*, 2013, pp. 2128–2131.

[15] S. H. Lloyd, G. A. Smith, and D. G. Infield, "Design and construction of a modular electronic photovoltaic simulator," in *Power Electronics and Variable Speed Drives, 2000. Eighth International Conference on (IEE Conf. Publ. No. 475)*, 2000, pp. 120–123.

[16] K. Khouzam, C. Ly, C. K. Koh, and P. Y. Ng, "Simulation and real-time modelling of space photovoltaic systems," in *IEEE Photovoltaic Specialists Conference - 1994, 1994 IEEE First World Conference on Photovoltaic Energy Conversion, 1994., Conference Record of the Twenty Fourth*, 1994, vol. 2, pp. 2038–2041 vol.2.

[17] D. Sera, R. Teodorescu, and P. Rodriguez, "PV panel model based on datasheet values," in *2007 IEEE International Symposium on Industrial Electronics*, 2007, pp. 2392–2396.

[18] H. Votzi, F. A. Himmelstoss, and H. Ertl, "Basic linear-mode solar-cell simulators," in *35th Annual Conference of IEEE Industrial Electronics*, 2009. IECON '09, 2009, pp. 261–265.

[19] A. Sanaullah and H. A. Khan, "Design and implementation of a low cost Solar Panel emulator," in *Photovoltaic Specialist Conference (PVSC), 2015 IEEE 42nd*, 2015, pp. 1–5.

[20] *Overall efficiency of grid connected photovoltaic inverters*, CENELEC, St. EN 50530, 2010.